17 February 1995

ELSEVIER

Chemical Physics Letters 233 (1995) 392–398

CHEMICAL PHYSICS LETTERS

Molecular vibrational state distributions in collisions

Jorge A. Morales, Agustín C. Diz, Erik Deumens, Yngve Öhrn

Quantum Theory Project, University of Florida, Gainesville, FL 32611-8435, USA

Received 18 October 1994; in final form 28 November 1994

Abstract

Experimental vibrational spectra of H_2 in the collision with a proton at 30 eV in the laboratory frame are compared to results from calculations using the electron nuclear dynamics. Nuclei are treated classically. Interpreting the classical vibration in terms of a coherent state yields quantum vibrational levels reproducing the experimental results. This result indicates that collision dynamics, including vibrational excitation, does not require numerical-grid wave packet dynamics for an understanding of the fundamental mechanisms involved, but that the concept of coherent state can provide a simple and accurate method to resolve product vibrational states from fully dynamical classical trajectories.

1. Introduction

Nuclear degrees of freedom in atomic collisions behave quite classically. In fact, differential cross sections for elastic scattering can be obtained from classical trajectories. The only place where this approximation breaks down is in the region of a rainbow angle. But already the early work of Ford and Wheeler [1] showed that a semiclassical correction could be made to the cross sections, computed from classical trajectories, near the rainbow to reproduce the quantum results. These corrections are made a posteriori on the classical calculations.

For vibrational excitations in collisions, early work by Doll and Miller [2] used the classical *S*-matrix approach to obtain transition probabilities to quantum vibrational states. Their results compare well to quantum approaches. Giese and Gentry [3] analyzed the vibrational excitation of H_2 using classical motion of the nuclei on the ground state surface of H_3^+. Their method (named DECENT) entails several approximations such as not allowing electronic excitation, charge transfer and nuclear exchange. The DECENT approach assumes a quadratic approximation to the H_2 surface, with a time-dependent force provided by the proton in the collision. Using the quantum-classical correspondence for a quadratic potential, the final quantum vibrational distribution is computed. A similar approach, but employing straight line trajectories, was presented by Krüger and Schinke [4].

Chemists and molecular physicists intuitively think of nuclei in molecules as being classical, with possible exception for the interpretation of rovibrational spectroscopy. One could pose the question whether similar a posteriori corrections can be achieved for classical vibrational motion to obtain the distribution over quantum states. In order to answer this question in some detail we use the classical nuclei approximation to study the product H_2 molecule after a collision with a proton having an initial laboratory kinetic energy of 30 eV.

This collision was experimentally studied by Niedner et al. [5]. Their theoretical analysis employs

Elsevier Science B.V.
SSDI 0039-6028(94)01472-8

the trajectory surface hopping model (TSH). Baer et al. [6,7] used the infinite order sudden approximation (IOSA) quantum approach to study this system. Both methods use two diabatic potential energy surfaces of H_3^+ obtained from a diatomics-in-molecules (DIM) approach. This DIM approach includes a representation of the nonadiabatic couplings between these surfaces.

Experiment shows a nearly exponential drop for the total cross sections for each vibrational state between vibrational quantum numbers $v = 0$ and $v = 6$. TSH, with a binning procedure not fully explained in this latter, fails to show this behavior, while Baer's IOSA results coincide with those of experiment. This would seem to indicate that a quantum model is necessary to understand vibrationally resolved spectra.

The $H^+ + H_2$ collision is studied using the electron nuclear dynamics (END) approach [8–10] at the simplest level of approximation, i.e. taking the limit of classical nuclei and a single determinental state for the electrons. The distinguishing feature of this approach is that it is a time-dependent theory, employing the time-dependent variational principle as the fundamental principle to derive the equations for the evolution of the electronic and nuclear parameters. The END theory uses the instantaneous forces between electrons and nuclei, and, thus, does not use a priori potential energy surfaces or the Born–Oppenheimer approximation. Electron–nuclear couplings are fully accounted for in the phase space metric of the equations. These couplings are very important to obtain correct results for dynamics of molecular systems [11]. The structure of the END equations is briefly discussed in Section 2.

Following similar ideas of Giese and Gentry [3] in order to compute the appropriate vibrational cross sections from the classical nuclear parameters, a coherent state analysis is carried out on the asymptotic part of a trajectory. However, no potential surface is assumed in the dynamics and charge transfer and other dynamical processes which were not considered in the original DECENT approach are included. Excitation levels up to $n = 6$ are computed and compared. The results show excellent agreement with experiment suggesting that in collisions, the nuclei behave by populating the vibrational states in a 'classical' fashion in the sense of coherent states. A longer paper in preparation analyzes other aspects of the dynamics of this system such as charge transfer and differential cross sections.

2. END theory

The ideas behind END are straightforward. The theory is discussed in great detail elsewhere [10] and so a brief overview suffices here.

The time-dependent variational principle (TDVP) is used as a unifying principle to derive the dynamic equations for the system parameters. The use of the TDVP allows the equations of motion to apply not only for a fully quantal or fully classical treatment, but also for a mixed quantum-classical equations of motion. For the full quantum approach, with a complete basis, the TDVP yields the time-dependent Schrödinger equation [12]. For a completely classical system, the TDVP is just the standard variational principle from which the classical Hamilton's equations are obtained. For basis functions which depend, in some form, on the classical parameters (e.g. basis functions centered on nuclei described classically), this approach exhibits nonadiabatic couplings between the classical and quantum degrees of freedom. These couplings are essential for satisfying conservation theorems and for correct behavior of many observable quantities [11,13].

Approximate dynamical equations are obtained by making specific choices of the form of wavefunctions and which degrees of freedom are to be treated classically. For this study the atomic nuclei are classical and the electronic basis functions are centered on the nuclei. A single Thouless determinant [14] is used to describe the electrons. The theory for more elaborate wavefunctions has been developed, but not implemented in a working code yet [15,16]. This approximation has been shown to provide a good description for many ion–atom and ion–molecule reactive collision processes [8,10,17].

The Lagrangian is

$$L = \tfrac{1}{2}\sum_k (\boldsymbol{P}_k \cdot \boldsymbol{R}_k - \boldsymbol{P}_k \cdot \boldsymbol{R}_k) - \sum_k \frac{\boldsymbol{P}_k^2}{2M_k} + \langle \Psi_{el} | \frac{i}{2}\left(\frac{d}{dt} - \frac{\tilde{d}}{dt}\right) - H_{el} | \Psi_{el} \rangle / \langle \Psi_{el} | \Psi_{el} \rangle, \quad (1)$$

where $\tilde{\mathrm{d}}/\mathrm{d}t$ acts on the bra and H_{el} contains the nuclear repulsion potentials. The TDVP requires

$$\delta \int L \, \mathrm{d}t = 0. \tag{2}$$

Dynamics requires the wavefunction to be complex so that the phase space for the electrons is well defined. Standard normalized molecular orbital (MO) coefficients are redundant, which can be seen from the fact that rotations among occupied and unoccupied states do not change the state. Such a choice of MO coefficients as dynamical parameters makes the equations singular. Thouless [14] recognized this and developed a set of nonredundant parameters z for a single determinant. They turn out to be the coset representatives of the group $U(K)$, where K is the rank of the basis. Single determinants parametrized this way are also known as coherent states [10,12,18]. The important features of these parameters from the point of view of dynamics is that they provide a complex, continuous, nonredundant parametrization, thus ensuring a proper (generalized) phase space for the electronic degrees of freedom.

In terms of a given spin-orbital basis set $\{\phi_i; i = 1, K\}$ centered on the nuclei, the occupied orbitals of the determinant are

$$\chi_h = \phi_h + \sum_{p=N+1}^{K} z_{ph}\phi_p. \tag{3}$$

The first N orbitals ϕ_h form the reference determinant. If the basis is orthogonal, the virtual dynamical orbitals are written in terms of the same coefficients as

$$\chi_p = \phi_p - \sum_{h=1}^{N} z_{ph}^{*}\phi_h. \tag{4}$$

In terms of a nonorthogonal basis the virtual dynamical orbitals are

$$\chi_p = \phi_p + \sum_{h=1}^{N} v_{hp}^{*}\phi_h, \tag{5}$$

where the v coefficients are functions of the complex, time-dependent z coefficients [8,10]. The orbitals χ_h are nonorthogonal as are χ_p, but satisfy $\langle \chi_p \mid \chi_h \rangle = 0$.

Having defined the dynamical parameters for electrons and nuclei, the TDVP yields

$$\begin{pmatrix} \mathrm{i}C & 0 & \mathrm{i}C_R & 0 \\ 0 & -\mathrm{i}C^{*} & -\mathrm{i}C_R^{*} & 0 \\ \mathrm{i}C_R^{\dagger} & -\mathrm{i}C^{\mathrm{T}} & C_{RR} & -I \\ 0 & 0 & I & 0 \end{pmatrix} \begin{pmatrix} \dot{z} \\ \dot{z}^{*} \\ \dot{\boldsymbol{R}} \\ \dot{\boldsymbol{P}} \end{pmatrix} = \begin{pmatrix} \partial E/\partial z^{*} \\ \partial E/\partial z \\ \partial E/\partial \boldsymbol{R} \\ \partial E/\partial \boldsymbol{P} \end{pmatrix}, \tag{6}$$

where the total energy is

$$E = \sum_{I} \frac{P_I^2}{2M_I} + \frac{\langle z \mid H_{\mathrm{el}} \mid z \rangle}{\langle z \mid z \rangle}. \tag{7}$$

The coupling elements in Eq. (6) are

$$C = \left. \frac{\partial^2 \ln S(z^{*}, \boldsymbol{R}', z, \boldsymbol{R})}{\partial z^{*} \partial z} \right|_{\boldsymbol{R}=\boldsymbol{R}'},$$

$$C_R = \left. \frac{\partial^2 \ln S(z^{*}, \boldsymbol{R}', z, \boldsymbol{R})}{\partial z^{*} \partial R} \right|_{\boldsymbol{R}=\boldsymbol{R}'},$$

$$C_{RR} = -2 \, \mathrm{Im} \left. \frac{\partial^2 \ln S(z^{*}, \boldsymbol{R}', z, \boldsymbol{R})}{\partial R' \partial R} \right|_{\boldsymbol{R}=\boldsymbol{R}'}. \tag{8}$$

They are derived from the overlap

$$S(z^{*}, \boldsymbol{R}', z, \boldsymbol{R}) = \langle z; R' \mid z; R \rangle \tag{9}$$

formed between Thouless determinants at different geometries R', R.

The TDVP ensures the conservation of important physical quantities such as total energy, total momentum and total angular momentum [8,10].

3. Vibrational analysis

It is well known that there are quasi-classical states in the theory of the harmonic oscillator whose expectation values of the position and momenta follow the classical equations of motion [19]. These are also called coherent states, different from the coherent state electronic wavefunction used in Section 2.

For a quantum oscillator with vibrational frequency ω, a vibrational coherent state is written as [20]

$$|\alpha\rangle = \exp\left(-\tfrac{1}{2}|\alpha|^2\right)\sum_n \frac{\alpha^n}{\sqrt{n!}}|n\rangle, \tag{10}$$

where $|n\rangle$ are the eigenstates of the oscillator Hamiltonian. The vibrational states therefore have a probability distribution

$$\exp(-|\alpha|^2)\frac{|\alpha|^{2n}}{n!}. \tag{11}$$

The coherent state expectation value of the energy is

$$E = \langle H\rangle = \hbar\omega\left(|\alpha|^2 + \tfrac{1}{2}\right). \tag{12}$$

The question can be posed whether, when the system is initially in the vibrational ground state, the product vibrational states follow a coherent state distribution. Should this be the case, then as long as the vibrational energy levels of interest are approximately equidistant, a classical trajectory approach can be used to determine the amount of energy put into classical vibrational excitation, and then compute the resulting distribution via coherent states. This is in effect the a posteriori quantum analysis of the classical vibrational energy in a collision. For low energy collisions of chemical interest, only the lowest vibrational states of a molecule are excited. These are well approximated by energy levels of constant separation.

The kinetic energy of the product molecule to be studied can be computed from the final total nuclear kinetic energy. Then subtracting the translational energy of the center of mass of this molecule results in the rovibrational kinetic energy. An estimate of the rotational energy for most trajectories using the moment of inertia at the equilibrium position shows that it is a small fraction of the total rovibrational kinetic energy for the $H^+ + H_2$ collision. This is demonstrated in Section 4. The product molecule energy in the center of mass system is obtained by projecting the electronic state of the compound system (of $H^+ + H_2$ in this case) onto that of the particular product molecule (H_2). The electronic energy of that projected state, possibly an electronically excited state of the product molecule, minus the ground state energy in the given basis gives the excitation energy, which, when added to the rovibrational kinetic energy, yields the energy available for quantum rotation and vibration of the product molecule in its electronic ground state.

Assuming that all of that energy is in the vibrational mode, then this energy E_v (which has had the zero-point energy already eliminated) is

$$E_v = \hbar\omega|\alpha|^2 \tag{13}$$

and so for a given trajectory the populations of the vibrational levels are

$$\exp(-E_v/\hbar\omega)\frac{(E_v/\hbar\omega)^n}{n!}. \tag{14}$$

This procedure is tested on the $H^+ + H_2$ system where the proton has an initial energy of 30 eV in the laboratory frame.

4. Results

A pVDZ basis consisting of two s and one p orbital (actually p_x, p_y, and p_z) centered on each nucleus is used. Past experience has shown this to give an excellent description for hydrogenic systems of this kind. The initial conditions of the collision uses two angles to define the relative orientation of the target H_2 molecule. When all the nuclei are in a plane the azimuthal angle ϕ is zero, and the angle θ defines the orientation of H_2 with respect to the initial direction of the incoming proton. The impact parameter of the projectile (H^+) assumes values between -6 and 6 au, from the center of mass of the H_2 in steps of 0.1 or 0.2 au depending on the dynamics. Initial values for θ of 0°, 15°, 30°, 45°, 60°, 75° and 90° and azimuthal angles ϕ of 0°, 45° and 90° were chosen. The cross sections are found by averaging over all the initial orientations. The integral over θ has a weight given by sin θ.

Table 1 shows the vibrational levels obtained from the pVDZ basis for H_2, the 'exact' vibrational levels obtained by Kolos and Wolniewicz [21] and what the first six levels are with a constant energy difference obtained from the harmonic fundamental frequency. As one would expect, a harmonic oscillator description is reasonable for the lowest states, but is inadequate for higher values of n.

Table 1
Vibrational levels of H_2. Exact values from Ref. [21]. Vibrational levels for the pVDZ basis using the method of Meyer [22], and assuming a constant (harmonic) separation with a fundamental frequency of 4477.4 cm^{-1}. All units in cm^{-1}

Vib. level	Exact	pVDZ basis	Harmonic
0	2174.7	2238.7	2238.7
1	6336.8	6615.6	6716.1
2	10263.4	10773.8	11193.5
3	13959.6	14698.7	15670.9
4	17428.2	18353.8	20148.3
5	20670.5	21613.6	24625.7
6	23685.0	24447.9	29103.1

The experimental setup [5] uses time-of-flight spectroscopy to determine the energy loss of the outgoing proton with respect to the incoming kinetic energy. The spectrum is then fitted to Gaussians. The Gaussian peaks fit the vibrational energy levels of H_2 well. The authors do note that there is a shift in the peak at higher vibrational levels and suggest that this may have to do with rotational excitation of the H_2 molecule. The Gaussians are then integrated to give relative values for the cross sections. The spectrum was measured for laboratory scattering angles between 0° and 12°.

The energy E_v is computed for each trajectory and the distribution obtained for each impact parameter. Since END does not impose restrictions on the dynamics of the nuclei, dissociation is allowed and happens, but these trajectories are excluded from the vibrational analysis. A cross section for a given orientation and vibrational level is computed by

$$\sigma(n;\,\theta,\,\phi) = \pi\int_{-\infty}^{\infty} P(H_2;\,b,\,\theta,\,\phi) \times P(n;\,b,\,\theta,\,\phi)\,|\,b\,|\,\mathrm{d}b,$$

$$P(n;\,b,\,\theta,\,\phi) = \exp[-E_v(\theta,\,\phi)/\hbar\omega] \times \frac{[E_v(\theta,\,\phi)/\hbar\omega]^n}{n!}, \qquad (15)$$

where $P(H_2;\,b,\,\theta,\,\phi)$ is the probability that charge was not transferred from H_2 to the proton, obtained by the projection of the electronic state. These cross sections are numerically averaged over initial conditions to get the final result, which is compared to experiment, i.e.

$$\sigma(n) = \int_0^{\pi/2}\mathrm{d}\theta\,\sin\theta\int_0^{\pi/2}\mathrm{d}\phi\,\sigma(n;\,\theta,\,\phi)\Big/ \int_0^{\pi/2}\int_0^{\pi/2}\sin\theta\,\mathrm{d}\theta\,\mathrm{d}\phi, \qquad (16)$$

where the symmetry of the molecule is used to reduce the angular ranges.

The results for vibrational levels 1 through 6 are shown in Fig. 1 compared with experiment and two other theoretical results, the TSH [5] and IOSA [7]. The experimental cross sections, which are only relative, have been normalized so that the first vibrational excitation coincides with END. The END results presented in this figure have been corrected by subtracting an estimate of the rotational kinetic energy from E_v. The estimate uses the moment of inertia for H_2 at the equilibrium bond distance plus the centrifugal distortion.

Fig. 2 shows the structure of E_v, with rotational energy subtracted, as a function of impact parameter

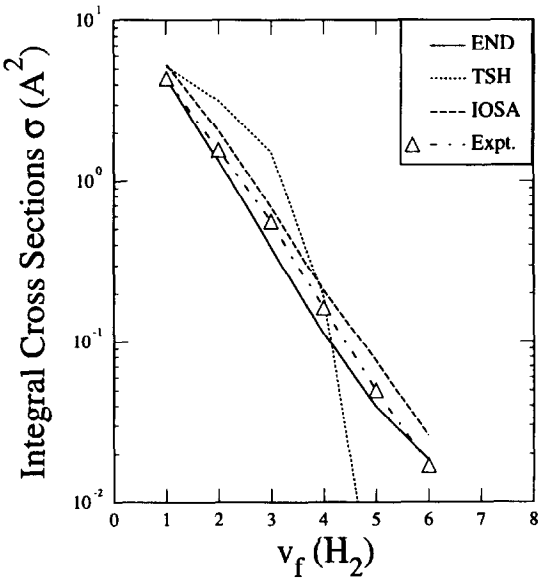

Fig. 1. Integral cross sections for vibrational excitation of H_2 in $H^+ + H_2(n=0) \rightarrow H^+ + H_2(n \neq 0)$. Experiment and TSH from Ref. [5]. IOSA from Ref. [7]. END results using the coherent state vibrational population expression on the energy remaining after subtracting translational kinetic energy, projecting wavefunction on H_2 state and subtracting estimate of rotational kinetic energy.

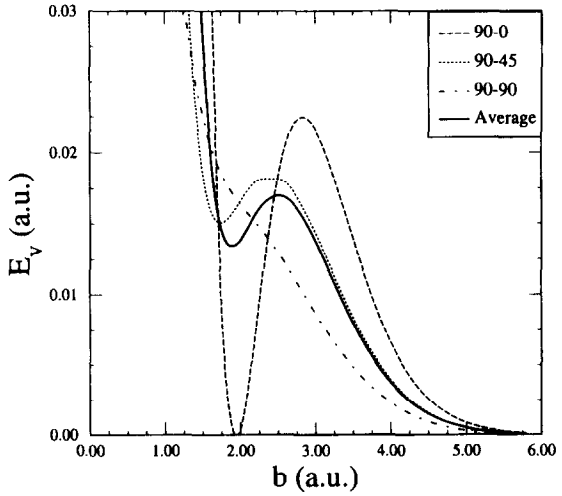

Fig. 2. Vibrational excitation energy of H_2 in $H^+ + H_2(n=0) \rightarrow H^+ + H_2(n \neq 0)$ as a function of impact parameter. Values for geometries of $\theta = 90°$ and $\phi = 0°$, 45° and 90° are shown, as well as the average over all values of θ and ϕ. Impact parameters of less than 1.4 au generally correspond to breakup channels. The hump around 2.5 au is associated with rainbow scattering. Other values of θ produce similar results to the ones shown, with the largest hump corresponding to $\phi = 0°$ and a lack of such for $\phi = 90°$.

for various initial geometries and, in a full thick line, the result of averaging over all orientations, not only those shown. Other values of θ show very similar characteristics as the ones shown here for $\theta = 90°$. The smaller impact parameters correspond mostly to breakup channels. The hump around $b = 2.5$ au is associated with the rainbow angle. The structure of these plots is similar to the results of Giese and Gentry [3].

Table 2 presents the numbers used in Fig. 1, along with cross sections computed when the estimate of the rotational energy is not subtracted. For the lower vibrational levels, both approaches (with and without rotational energies) are essentially the same. A clear effect is seen for higher vibrational levels.

Table 2
Total cross sections for vibrational excitation in $H^+ + H_2(n=0) \rightarrow H^+ + H_2(n \neq 0)$. Experiment and TSH taken from Fig. 9 in Ref. [5], END 1 and END 2 are present results. END 1 has had an estimate of the rotational energy subtracted from the remaining rovibrational energy. END 2 is using all of the rovibrational energy. IOSA from Table I in Ref. [7], for laboratory scattering angles between 0–12° (0–18° in the c.m.)

Vib. state	Exp.	END 1	END 2	TSH	IOSA
1	4.3	4.35	4.35	5.2	5.3
2	1.6	1.33	1.43	3.2	2.06
3	0.56	0.386	0.47	1.5	0.68
4	0.16	0.112	0.160	0.2	0.209
5	0.050	0.040	0.062	0.002	0.076
6	0.017	0.018	0.027	–	0.026

5. Conclusions

The differences with the TSH results are striking. The END results using the coherent state distribution give the nearly exponential drop that experiment measures. The IOSA results are larger than END by about 30%. It would be interesting to get new reliable experiments that measure the absolute cross sections. The results found by Baer et al. [7] may be artificially high because in their IOSA approach the breakup channel is excluded and probability that would flow into this channel is being artificially retained in other channels. The differences between the IOSA results and the END results may be smaller than the experimental error. The rotational kinetic energy is of some importance for higher vibrational levels, but not overwhelmingly so, for this system.

These results show that the classical nuclear trajectories, when determined in a fully dynamical fashion carry all the necessary information to yield the distribution over quantum levels. This is in itself interesting, in the sense that a coherent state interpretation of the classical evolution correctly predicts the distribution over quantum levels.

Although this is a simple system, with only one vibrational mode, the ideas can be extended readily to a system with several vibrational modes. The x, y and z components of the asymptotic part of the trajectory for a fragment with N rovibronic modes, with the translational motion eliminated, are analyzed in a finite Fourier series with N terms. This results in N frequencies, since all Cartesian components have the same frequency content, and $3N$ weights. The weights define the transformation matrix to the normal modes. The relative weight of each of the normal modes in the asymptotic part of the trajectory can be obtained by transformation to the

normal modes of one configuration. The same procedure as used here for the single mode system is then implemented. First one estimates the rotational energy using the inertia tensor of the fragment at any configuration on the asymptotic part of the trajectory. Then the vibrational energy is identified with the energy of a multidimensional oscillator coherent state, with the frequencies and modes found by the finite-mode Fourier analysis. This effectively partitions the vibrational energy into N parts. The probability for each level is then found by using the distribution in Eq. (14) for all modes. To obtain total cross sections averaging over all orientational angles must be carried out as usual.

Acknowledgement

This work was supported by a grant from the Office of Naval Research. We thank Benny J. Mogensen for providing us with the program to compute vibrational levels using Meyer's approach.

References

[1] K.W. Ford and J.A. Wheeler, Ann. Phys. 7 (1959) 259.
[2] J.D. Doll and W.H. Miller, J. Chem. Phys. 57 (1972) 5019.
[3] C.F. Giese and W.R. Gentry, Phys. Rev. A 10 (1974) 2156.
[4] H. Krüger and R. Schinke, J. Chem. Phys. 66 (1977) 5087.
[5] G. Niedner, M. Noll, J. Toennies and Schlier, J. Chem. Phys. 87 (1987) 2686.
[6] M. Baer, G. Niedner and J.P. Toennies, J. Chem. Phys. 88 (1988) 1461.
[7] M. Baer, G. Niedner-Schatteburg and J.P. Toennies, J. Chem. Phys. 91 (1989) 4169.
[8] E. Deumens, A. Diz, H. Taylor and Y. Öhrn, J. Chem. Phys. 96 (1992) 6820.
[9] Y. Öhrn et al., in: Time-dependent quantum molecular dynamics, eds. J. Broeckhove and L. Lathouwers (Plenum Press, New York, 1992) pp. 279–292.
[10] E. Deumens, A. Diz, R. Longo and Y. Öhrn, Rev. Mod. Phys. 66 (1994) 917.
[11] R. Longo, A. Diz, E. Deumens and Y. Öhrn, Chem. Phys. Letters 220 (1994) 305.
[12] P. Kramer and M. Saraceno, Geometry of the time-dependent variational principle in quantum mechanics (Springer, Berlin, 1981).
[13] A. Diz and Y. Öhrn, Intern. J. Quantum Chem. Symp. 28 (1994), in press.
[14] D.J. Thouless, Nucl. Phys. 21 (1960) 225.
[15] E. Deumens, Y. Öhrn and B. Weiner, J. Math. Phys. 32 (1991) 1166.
[16] B. Weiner, E. Deumens and Y. Öhrn, J. Math. Phys. 35 (1994) 1139.
[17] R. Longo, E. Deumens and Y. Öhrn, J. Chem. Phys. 99 (1993) 4554.
[18] J.R. Klauder and B.-S. Skagerstam, Coherent states, applications in physics and mathematical physics (World Scientific, Singapore, 1985).
[19] E. Schrödinger, Naturwissenschaften 14 (1926) 664.
[20] C. Cohen-Tannoudji, B. Diu and F. Laloë, Quantum mechanics, Vol. 1 (Wiley–Interscience, New York, 1977).
[21] W. Kołos and L. Wolniewicz, J. Chem. Phys. 49 (1968) 404.
[22] R. Meyer, J. Chem. Phys. 52 (1970) 2053.